This manuscript was accepted and published by ***Energy & Fuels***, a journal of the American Chemical Society. DOI: 10.1021/ef4016075 (http://dx.doi.org/10.1021/ef4016075).

This manuscript was placed into the present public repository with the consent of the Editor of *Energy & Fuels*. Publication data of the final, corrected work:

Tapasvi, D.; Khalil, R.; Várhegyi, G.; Tran, K.-Q.; Grønli, M.; Skreiberg, Ø.: Thermal decomposition kinetics of woods with an emphasis on torrefaction. Energy Fuels, **2013**, 27, 6134-6145. doi: 10.1021/ef4016075

Thermal Decomposition Kinetics of Woods with Emphasis on Torrefaction

Dhruv Tapasvi,[†] Roger Khalil,[‡] Gábor Várhegyi,[,§] Khanh-Quang Tran,[†] Morten Grønli,[†] and Øyvind Skreiberg[‡]*

[†]Department of Energy and Process Engineering, Norwegian University of Science and Technology (NTNU), NO-7491 Trondheim, Norway

[‡]SINTEF Energy Research, Postboks 4761 Sluppen, NO-7465 Trondheim, Norway

[§]Institute of Materials and Environmental Chemistry, Research Centre for Natural Sciences, Hungarian Academy of Sciences, PO Box 17, Budapest, Hungary 1525

KEYWORDS: Birch; spruce; pyrolysis kinetics; thermogravimetry; torrefied wood; distributed activation energy model.

ABSTRACT. The pyrolysis kinetics of Norwegian spruce and birch wood was studied to obtain information on the kinetics of torrefaction. Thermogravimetry (TGA) was employed with nine different heating programs, including linear, stepwise, modulated and constant reaction rate (CRR) experiments. The 18 experiments on the two feedstocks were evaluated simultaneously by the

method of least squares. Part of the kinetic parameters could be assumed common for both woods without a considerable worsening of the fit quality. This process results in better defined parameters and emphasizes the similarities between the woods. Three pseudocomponents were assumed. Two of them were described by distributed activation energy models (DAEM), while the decomposition of the cellulose pseudocomponent was described by a self-accelerating kinetics. In another approach all the three pseudocomponents were described by *n*-order reactions. Both approaches resulted in nearly the same fit quality but the physical meaning of the model based on three *n*-order reactions was found to be problematic. The reliability of the models was tested by checking how well the experiments with higher heating rates can be described by the kinetic parameters obtained from the evaluation of a narrower subset of 10 experiments with slower heating. A table of data was calculated that may provide guidance about the extent of devolatilization at various temperature – residence time values during wood torrefaction.

1. INTRODUCTION

There is a growing interest in lignocellulosic biomass fuels and raw materials due to climate change problems. However, the widespread use of biomass fuels is frequently hindered by their unfavorable fuel characteristics like high moisture content, poor grindability, low calorific value and low bulk density. Torrefaction is one of the potential solutions to these problems and it has gained research momentum as a biomass pre-treatment process in the last two decades. It results in improved biomass fuel properties such as reduced moisture content, higher energy density, improved hydrophobic behavior, and less energy consumption during grinding.[1-3] Torrefaction is typically conducted at 200–300°C, at atmospheric pressure, in the absence of oxygen and with particle heating rates below 50°C/min.[4] The lignocellulosic biomass is partly decomposed during

the torrefaction releasing condensable liquids and non-condensable gases into the gas phase.[5] Primarily the xylan-containing hemicellulose polymers decompose because they are the most reactive polymer structures in biomass.[6,7] The extractives of the biomass also decompose while the cellulose and lignin are moderately impacted during torrefaction, depending on the feedstock composition and the torrefaction temperature.[8]

Many studies are available on the production and characterization of torrefaction products. Fewer works deal with the torrefaction kinetics, however.[9-15] Most of these studies are based on isothermal experiments. Prins et al.[9] and Bates et al.[11] employed a one component, two step successive reaction model based on an earlier work of Di Blasi and Lanzetta[16] on xylan kinetics. The same model was used in a recent TGA-MS study by Shang et al.[15] Peng et al.[12] used a one component, one-step reaction model for torrefaction with long residence time and a two component, one-step reaction model for torrefaction with short residence time. Chen and Kuo[10] studied the torrefaction of hemicelluloses, cellulose and lignin separately using a global one-step reaction model for each. They described the torrefaction process of a biomass material by superimposed kinetics of the three components.

The torrefaction kinetics is part of a broader subject: the pyrolysis kinetics of biomass materials. If a kinetic model describes well the biomass pyrolysis, then it can obviously be used for torrefaction kinetics. Moreover, such a model can describe the pyrolysis behavior of the torrefied wood, too, if the experimental data used for the determination of the model parameters include temperature programs where the heating to higher temperatures is preceded by longer residence times in the temperature domain of the torrefaction. This way was followed in the present work. Such kinetic descriptions will be presented which describe well both the lower and the higher temperature regions of the wood pyrolysis. The work is based on thermogravimetric (TGA) experiments, because TGA is a high-precision method that provides well defined conditions in the kinetic regime. The highest

heating rate of the study was 40°C/min at which the decomposition terminated around 600°C. We did not employ isothermal kinetics because the concept "isothermal" involves a substantial transient time which is lost from the evaluation of the thermogravimetric experiments. Though an "isothermal" experiment is involved in the study, it is evaluated together with the heat-up period. The information content of an essentially non-isothermal series of experiments was used to draw dependable kinetic information.

Due to the complex composition of biomass materials, the conventional linearization techniques of the non-isothermal kinetics are not suitable for the evaluation of the TGA experiments. Therefore the TGA experiments of biomass materials are usually evaluated by the non-linear method of least squares, assuming more than one reaction.[17-19] Biomass fuels and residues contain a wide variety of reactive species. The assumption of a distribution in the reactivity of the decomposing species frequently helps the kinetic evaluation of the pyrolysis of complex organic samples.[20] The distributed activation energy models (DAEM) have been used for biomass pyrolysis kinetics since 1985, when Avni et al. applied a DAEM for the formation of volatiles from lignin.[21] Several variants of DAEMs are known; usually a Gaussian distribution of the activation energy is employed. The use of DAEM in pyrolysis research was subsequently extended to a wider range of biomasses and materials derived from plants. Due to the complexity of the investigated materials the model was expanded to simultaneous parallel reactions (pseudocomponents) that were described by separate DAEMs.[22-25] The increased number of unknown model parameters required the least squares evaluation of larger series of experiments with linear and non-linear temperature programs.[22,26-29] The model parameters obtained in this way allowed accurate prediction outside the domain of the experimental conditions of the given kinetic evaluations.[22,26,28,29] The prediction tests helped to confirm the reliability of the model.

The complex decomposition of the biomass pseudocomponents can be approximated formally by *n*-order (power-law) kinetics, too. Manyà et al. proved that third order kinetics gives a better description for the lignin pseudocomponent of the biomass than the simpler first order kinetics.[30] Conesa and Domene showed the applicability of high reaction orders (up to 9.5) for the formal description of the pseudocomponents in biomass pyrolysis kinetics.[19] The aims of the present work included a careful comparison of the DAEM and the *n*-order approaches on a particularly wide domain of temperature – time functions.

2. SAMPLES AND METHODS

2.1 Samples. Birch and spruce samples were taken from standard Norwegian construction boards. Table 1 shows the proximate and ultimate analyses, and the higher heating values of the samples. A recent work of Tapasvi et al.[3] lists the corresponding data for the torrefied products prepared from the same woods. Before the experiments, the samples were cut into smaller pieces and ground in a cutting mill that was equipped with a 1 mm bottom sieve. The samples were sieved afterward and the particles in the range of 63-125 μm were used for the kinetic study.

Table 1: Proximate and ultimate analyses of the samples

Sample	Proximate analysis[a]			Ultimate analysis[a]					HHV[b]
	VM	fC	Ash	C	H	O	N	S	
Birch	89.4	10.4	0.2	48.62	6.34	44.90	0.09	< 0.05	19.80
Spruce	86.3	13.4	0.2	50.10	6.36	43.52	0.07	< 0.05	20.45

[a] % (m/m), dry basis. [b] Higher heating value, MJ/kg, dry basis.

2.2 Experimental Setup and Procedure. The experiments were carried out by a Q5000 IR analyzer from TA Instruments which has a sensitivity of 0.1 μg. High purity nitrogen was used as

purge gas with a gas flow of 100 mL/min. The initial sample mass was between 3 and 10 mg. The samples of both woods were analyzed with nine different heating programs, as shown in Figure 1. The linear T(t) experiments had heating rates of 40, 20, 10 and 5°C/min. The isothermal experiment with 30 min residence time at 275°C mimicked the T(t) of the actual torrefaction experiments used in earlier works.[3,31] In the modulated experiments sinus waves with 5 °C amplitudes and 200 s wavelength were superposed on a slow, 2 °C/min linear T(t). They served to increase the rather limited information content of the linear T(t) experiments. In the "constant reaction rate" (CRR) experiments the equipment regulated the heating of the samples so that the reaction rate would oscillate around a preset limit.[32] The CRR experiments aimed at getting very low mass-loss rates in the whole domain of the reaction. The highest mass loss rate was found to be 0.8 μg/s in these experiments. This value corresponds to 0.8×10^{-4} s^{-1} after normalization by the initial dry sample mass. The T(t) program for a CRR experiment obviously depends on the behavior of the given sample. Two stepwise temperature programs were employed which also served to increase the amount of experimental information for the kinetic evaluation.[22,26-29]

Figure 2 shows a test on the employed sample masses. The comparison of experiments with 3 and 10 mg initial sample masses (solid and dashed curves) indicates that the enthalpy change of the decomposition does not result in a considerable thermal lag at the higher sample mass. Figure 2 also compares the decomposition of the birch and spruce samples (red and blue lines). One can see that the low temperature partial peak, around 280-300°C, is more separated in the case of the birch sample. This is a usual difference between hardwoods (angiosperm trees) and conifers.[33] The main peak, belonging to the cellulose decomposition,[33] is very similar; its peak maximum occurs around 383°C for both samples in Figure 2.

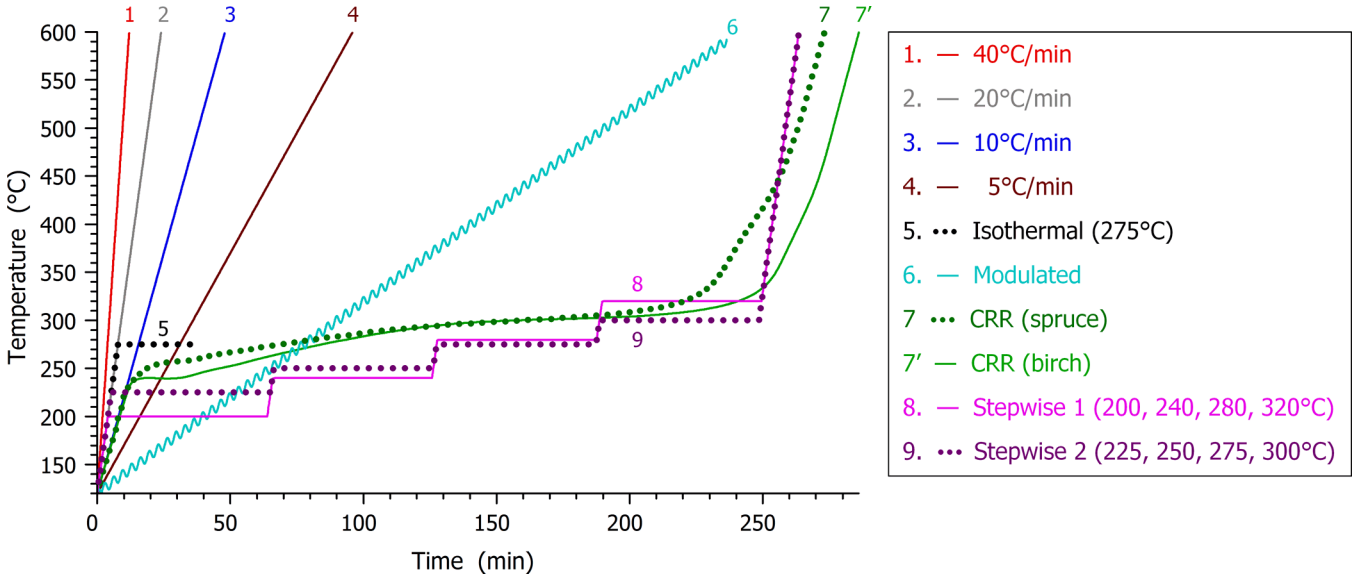

Figure 1. Temperature programs used in the TGA experiments. Note that the T(t) needed for a nearly constant heating rate in the CRR experiments was determined by the instrument and differed for the two samples.

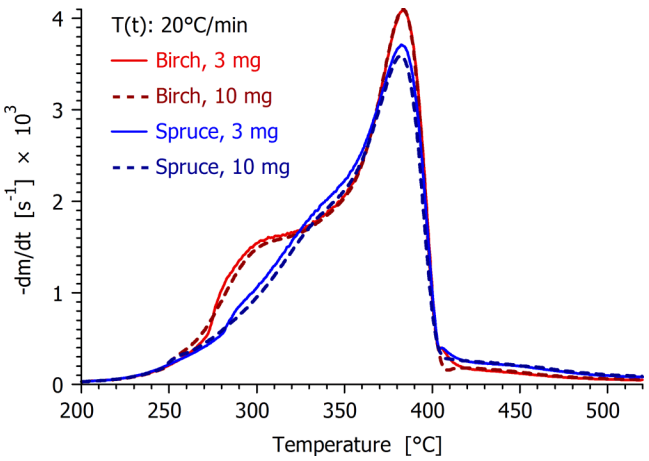

Figure 2. A test on the effect of sample mass and the comparison of the birch and spruce decomposition at 20°C/min heating rate.

2.3. Kinetic Evaluation by the Method of Least Squares and Characterization of the Fit Quality. Fortran 95 and C++ programs were used for the numerical calculations and for graphics

handling, respectively. The employed numerical methods have been described in details earlier.[27] The kinetic evaluation was based on the least squares evaluation of the $-dm^{obs}/dt$ curves, where m^{obs} is the sample mass normalized by the initial dry sample mass. The method used for the determination of $-dm^{obs}/dt$ does not introduce considerable systematic errors into the least squares kinetic evaluation of experimental results.[34] The model was solved numerically along the empirical temperature – time functions. The minimization of the least squares sum was carried out by a direct search method, as described earlier.[27] Such values were searched for the unknown model parameters that minimized the following objective function (*of*):

$$of = \sum_{k=1}^{N_{exper}} \sum_{i=1}^{N_k} \frac{\left[\left(\frac{dm}{dt}\right)_k^{obs}(t_i) - \left(\frac{dm}{dt}\right)_k^{calc}(t_i)\right]^2}{N_k h_k^2} \quad (1)$$

Here N_{exper} is the number of experiments evaluated together; its value is 18 in the present work. N_k denotes the number of t_i time points on a given curve and m is the sample mass normalized by the initial dry sample mass. The division by h_k^2 serves to counterbalance the high magnitude differences. Traditionally h_k is the highest observed value of the given experiment:

$$h_k = \max\left(\frac{dm}{dt}\right)_k^{obs} \quad (2)$$

The normalization by the highest observed values in the least squares sum assumes implicitly that the relative precision is roughly the same for the different experiments. This assumption has proved to be useful in numerous works on non-isothermal kinetics since 1993.[35] A recent work[31] deviated from this rule because the extremely low mass loss rates of the CRR experiments, 0.04–0.07 µg/s corresponded to a worse relative precision than the rest of the experiments. In the present work, however, we did not have so low mass loss rates; the peak maxima of the CRR experiments were >10 times higher, 0.8 µg/s, while most of the decomposition occurred at mass loss rates of 0.5 µg/s in these experiments.

The obtained fit quality can be characterized separately for each of the experiments evaluated together. For this purpose the relative deviation (*reldev*, %) will be used. The root mean square (rms) difference between the observed and calculated values is expressed as percent of peak maximum. For experiment *k* we get:

$$reldev\,(\%) = 100 \left\{ \sum_{i=1}^{N_k} \frac{\left[\left(\frac{dm}{dt}\right)_k^{obs}(t_i) - \left(\frac{dm}{dt}\right)_k^{calc}(t_i)\right]^2}{N_k h_k^2} \right\}^{0.5} \quad (3)$$

The fit quality for a given group of experiments is characterized by the root mean square of the corresponding relative deviations. The relative deviation of the 18 experiments evaluated together can be expressed by equations 1 – 3 as

$$reldev_{18}\,(\%) = 100\sqrt{of} \quad (4)$$

Obviously a smaller $reldev_{18}$ value indicates a better fit.

2.4. Distributed Activation Energy Model (DAEM). As outlined in the *Introduction,* a model of parallel reactions with Gaussian activation energy distribution was chosen as a starting point because favorable experience has been obtained by this type of modeling on similarly complex materials.[22-29] According to this model the sample is regarded as a sum of *M* pseudocomponents, where *M* is usually between 2 and 4. Here a pseudocomponent is the totality of those decomposing species which can be described by the same reaction kinetic parameters in the given model. A pseudocomponent may involve a large number of different reacting species. The reactivity differences are described by different activation energy values. On a molecular level each species in pseudocomponent *j* is assumed to undergo a first-order decay. The corresponding rate constant (*k*) is supposed to depend on the temperature by an Arrhenius formula. Let $\alpha_j(t,E)$ be the solution of the corresponding first order kinetic equation at a given *E* and *T(t)* with conditions $\alpha_j(0,E)=0$ and $\alpha_j(\infty,E)=1$:

$$d\alpha_j(t,E)/dt = A_j\, e^{-E/RT}\,[1-\alpha_j(t,E)] \quad (5)$$

The distribution of the species differing by E within a given pseudocomponent is approximated by a Gaussian function with mean value E_j and width-parameter (variation) σ_j. From a computational point of view, the approximate solution of a DAEM can simply be calculated from a discrete set of $\alpha_j(t,E)$ functions.[36] The normalized sample mass and its derivative are the linear combinations of $\alpha_j(t)$ and $d\alpha_j/dt$, respectively:

$$-dm/dt = \sum_{j=1}^{M} c_j\, d\alpha_j/dt \quad \text{and} \quad m(t) = 1 - \sum_{j=1}^{M} c_j \alpha_j\,(t) \quad (6)$$

where a weight factor c_j is equal to the amount of volatiles formed from a unit mass of pseudocomponent j.

This model will be called Model Variant **I** in the later treatment. Its modifications will be denoted by Model Variants **II** and **III**, as outlined in Sections 3.1 and 3.3. Finally the results were compared to a simpler, but more formal approximation, in which the decomposition of the pseudocomponents was described by n-order reactions:

$$\frac{d\alpha_j}{dt} = A_j \exp\left(-\frac{E_j}{RT}\right)\,(1-\alpha_j)^{n_j} \quad (j=1, 2, 3) \quad (7)$$

This n-order model will be referred as Model Variant **IV** in the treatment.

3. RESULTS AND DISCUSSION

3.1. Evaluation by Assuming Distributed Activation Energy Model for the Pseudocomponents. Based on earlier experience with this model,[26,28,29] and keeping in mind the shape of the DTG curves at linear heating programs (as shown by Figure 2), three pseudocomponents were assumed. The first describes mainly the decomposition of the hemicelluloses; the second corresponds to the cellulose decomposition, and the third would be

responsible for the long, flat tailing that can be observed at linear heating rates for nearly all biomasses. The graphical representation of these pseudocomponents will be shown in Sections 3.4 and 3.5. The width of distribution of the second reaction converged to zero, which means a 1st order kinetics. (The Gaussian distribution is a well-known Dirac delta function, hence a zero width cuts out a single reaction from the multitude of first order reactions.) Therefore the results of Model Variant **I** will be referred as "2DAEMs + 1st order cellulose" in the treatment. In Model Variant **II** the cellulose decomposition was described by an *n*-order reaction. This approach resulted in much better fit qualities, as shown in Section 3.2. The reaction order, n_2, was around 0.6. Model Variant **II** will be referred as "2DAEMs + *n*-order cellulose" in the treatment. A further modification of the cellulose decomposition kinetics is presented in Section 3.3.

3.2. Evaluation by Assuming Common Parameters. If part of the model parameters is assumed to be common for both samples, two benefits can be achieved:

(i) The common parameters indicate the similarities in the kinetic behavior of the samples;

(ii) A given parameter value is based on more experimental information; hence it is less dependent on the various experimental uncertainties.

The basic case is Evaluation **1** where none of the parameters was assumed to be common. It turned out that the fit quality depends only slightly on the exact choice of the values of E_3 and σ_3, hence these parameters could be forced to have identical values for both woods with only a slight worsening of the fit qualities. This behavior can be attributed to the ill-defined nature of pseudocomponent 3. As the green curve in Figure 3 shows, it is a wide and flat partial peak. A major part of this peak overlaps with the temperature domains of the first and second pseudocomponents. A change of the curve in this domain can be compensated by relatively small changes in the parameters of pseudocomponents 1 and 2. The situation was similar in two recent

works describing biomass pyrolysis by DAEMs.[28,29] The existence of various ill-definition problems (compensation effects) is well known in non-isothermal reactions. A similar problem was reported by de Jong et al. in 2007 for DAEMs.[37] The assumption of a common E_3 for both woods is denoted as Evaluation **2**, while the assumption of common E_3 and σ_3 for both woods is called Evaluation **3**.

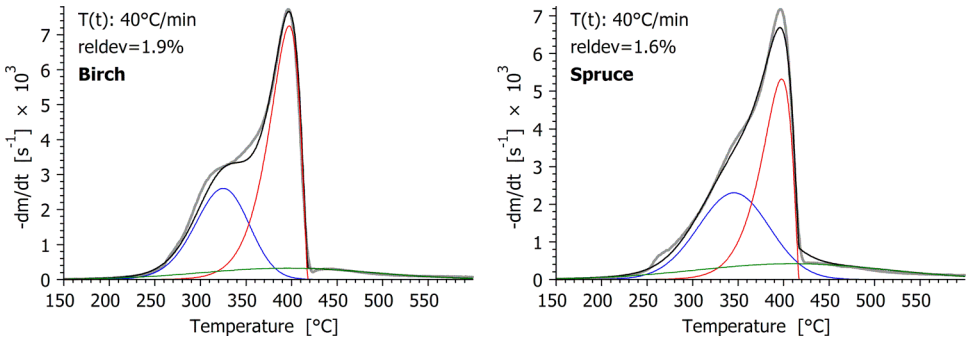

Figure 3. The partial peaks at 40°C/min obtained by Evaluation **1** and Model Variant **II**. Curves shown in the figure: observed and calculated –dm/dt (gray and black); peaks of pseudocomponents 1, 2, and 3 (blue, red and green).

The decomposition of the cellulose component resulted in similar E_2 and n_2 values for both woods. (The cellulose decomposition will be treated in details in later sections.) Accordingly these parameters could also be forced to have common values (Evaluation **4**). Finally we mention that the kinetics of the hemicellulose pyrolysis could also be described by identical E_1 and σ_1 parameters with some loss in the fit quality (Evaluation **5**). Table 2 shows the fit quality and the number of unknown parameters at the various model variants and evaluation strategies. Model variants **III** and **IV** will be discussed in later sections.

Table 2: Fit qualities[a] and the number of unknown parameters[b] at four model variants assuming various groups of common model parameters

Evaluation	Common parameters	Model variant			
		I 2 DAEMs + 1st order cellulose	**II** 2 DAEMs + *n*-order cellulose	**III** 2 DAEMs + accelerating cellulose[c]	**IV** 3 *n*-order reactions[d]
1	none	4.78 (22)	2.31 (24)	2.06 (26)	2.19 (24)
2	E_3	4.78 (21)	2.35 (23)	2.10 (25)	2.21 (23)
3	E_3, σ_3 or n_3[e]	4.78 (20)	2.37 (22)	2.14 (24)	2.21 (22)
4	E_3, σ_3 or n_3, E_2, n_2, z_2[e]	4.80 (19)	2.46 (20)	2.25 (21)	2.32 (20)
5	all except the A and c parameters	4.83 (17)	2.61 (18)	2.37 (19)	2.33 (18)

[a] $reldev_{18}$ (%) values are listed which characterize the fit quality of the whole series of experiments, as shown by equations 1 – 4. [b] The total number of the parameters determined by the method of least squares for the two biomasses is indicated in parentheses. [c] See Section 3.3. [d] See Section 3.6. [e] σ_3 belongs to Model variants **I**, **II** and **III** while n_3 corresponds to model variant **IV**. Parameter z_2 will be introduced in Section 3.3.. (z_2 occurs only in Model Variant **III**.)

3.3. Kinetics of the Cellulose Decomposition. In inert atmosphere, under the conditions of thermal analysis the cellulose decomposition is usually approximated by first order kinetics. In the present work *n*-order kinetics with $n_2 \approx 0.6$ gave considerable better fit quality than the first order kinetics, as mentioned above. More complex models are also employed in the literature. Among others, the use of self-accelerating kinetics has been suggested by Conesa et al.[38] and Capart et al.[39] In the presence of oxygen the cellulose decomposition was also found to be a self-accelerating reaction in recent studies based on evaluation strategies similar to the present work.[40,31] The self-accelerating reactions can typically be described by an equation of type

$$\frac{d\alpha_2}{dt} = A_2 \exp(-\frac{E_2}{RT})\, f(\alpha_2) \quad (8)$$

where f is a function capable of expressing self-acceleration. The mathematical unambiguity requires a normalization for $f(\alpha_2)$ because f functions differing only in constant multipliers are equivalent in eq 8 (parameter A_2 can compensate any multipliers of f). As a normalization, we require that the maximum of f be 1. $f(\alpha_2)$ is approximated formally by

$$f(\alpha_2) \cong normfactor\ (1-\alpha_2)^{n_2}\,(\alpha_2+z_2) \quad (9)$$

where n_2 and z_2 are model parameters, and *normfactor* ensures that max f=1. Parameters n_2 and z_2 do not have separate physical meaning; together however they determine the shape of f, and, in this way, the self-accelerating capabilities of the model. Eq 9 is a slightly simplified version of an earlier approximation that has been employed to different self-accelerating reactions.[41,40] In the present work $f(\alpha_2)$ reached its maximum at α_2 values between 0.05 – 0.15. The results obtained by the use of eq 9 are indicated as Model Variant **III** in the treatment. Table 2 indicates that the use of eq 9 instead of n-order kinetics decreases $reldev_{18}$ by 0.21 – 0.25. This gain in the fit quality is obtained by two extra parameter values in Evaluations **1** – **3** (a z_2 value for birch and another z_2 value for spruce) and one extra parameter value in Evaluations **4** – **5** (a common z_2 for both woods). We cannot determine the statistical significance of this decrease because the experimental errors of the thermal analysis data are neither independent nor random. Nevertheless, the observed changes in $reldev_{18}$ are higher than the other changes in $reldev_{18}$ within Model Variant **II**. Accordingly, the results of Model Variant **III** were selected for a detailed presentation in the next section.

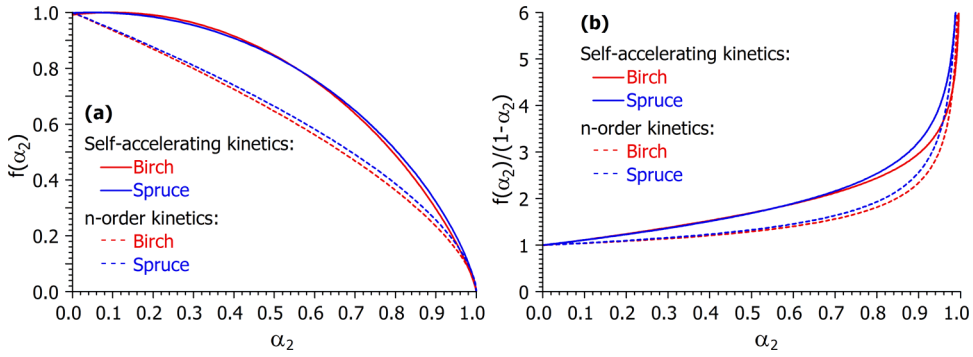

Figure 4. $f(\alpha_2)$ functions **(a)** and $f(\alpha_2)/(1-\alpha_2)$ ratios **(b)** obtained in Evaluation **3** by assuming self-accelerating kinetics (Model Variant **III**, solid lines) and *n*-order kinetics (Model Variant **II**, dashed lines) for the decomposition of the cellulose pseudocomponent.

Figure 4a compares the $f(\alpha_2)$ functions obtained by eq 9 (solid lines) to the ones obtained by *n*-order kinetics [$f(\alpha_2)=(1-\alpha_2)^{n_2}$, dashed lines].

The amount of the available cellulose is proportional to $1-\alpha_2$, hence the reaction rate of a unit mass of cellulose, i.e. the intrinsic reactivity of the sample is proportional to $f(\alpha_2)/(1-\alpha_2)$. When this quantity increases with α_2, as shown in Figure 4b, the intrinsic reactivity of the sample is increasing at constant T. $f(\alpha_2)/(1-\alpha_2)$ is obviously increasing with α_2 if $f(\alpha_2)=(1-\alpha_2)^{n_2}$ and $n_2<1$. When $f(\alpha_2)=(1-\alpha_2)^{n_2}$ is plotted as a function of α_2, the curve has a slight concave curvature, as the dashed lines in Figure 4a show. However, the *n*-order kinetics has only a limited ability to express kinetics with increasing intrinsic reactivity.

3.4. The Results of Evaluation 3 assuming Model Variant III. As outlined above, common E_3 and σ_3 values were assumed for both woods in Evaluation **3** due to the ill-defined nature of these parameters, while the decomposition of the cellulose pseudocomponents was described by eq 9 in Model Variant **III**. Figure 5 and 6 illustrate the corresponding results for the birch and spruce

experiments, respectively. These figures show the variety of the experiments demonstrating that the present study is based on a wider range of experiments than its predecessors.[28,29] The scaling of the vertical axes is particularly noteworthy. The peak maximum of $-dm/dt$ at T(t) program **1** (40°C/min) is nearly a hundred times higher than at T(t) program **7** (CRR).

Figures 5 and 6 contain the observed and calculated –dm/dt curves (gray and black bold lines); the contributions of the three pseudocomponents to the calculated –dm/dt (blue, red and green lines), and the non-isothermal T(t) functions, too, when appropriate (thin green line). The relative deviation (rms difference between the observed and calculated points) is also displayed. These values are around 1 and 2 % except the CRR experiments where the relative deviation is 5.1 and 4.2%. However, the height of the CRR curves is very low; hence the higher relative deviations correspond to very low deviations between the unnormalized mass loss rate data: 0.04 and 0.03 μg/s for the birch and spruce samples, respectively. It is possible that these low deviations are near to the experimental uncertainty of the CRR experiments.

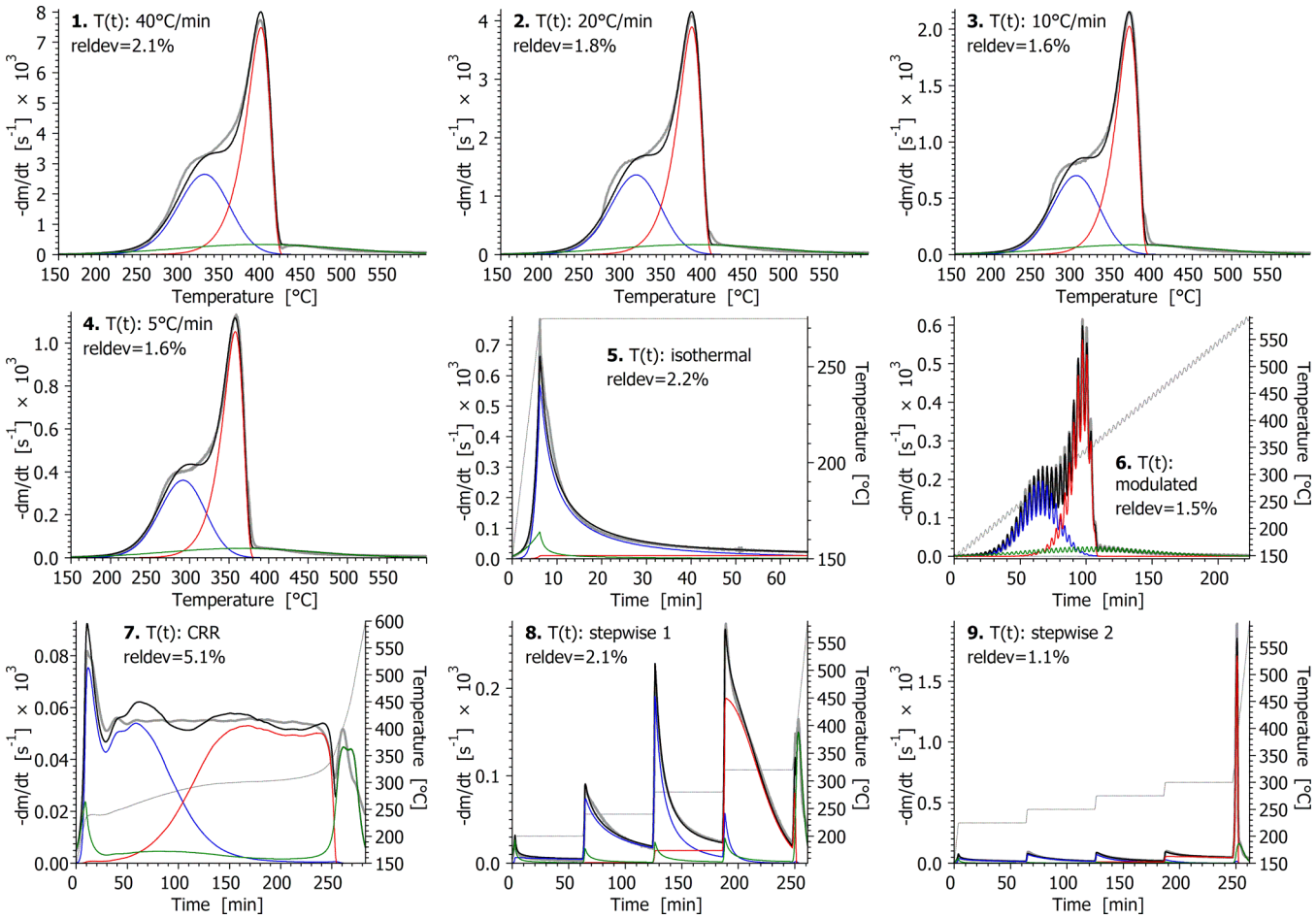

Figure 5. Results obtained for the birch experiments by Evaluation **3** and Model Variant **III**. Curves shown in the figure: observed and calculated –dm/dt (gray and black bold lines); peaks of pseudocomponents 1, 2, and 3 (blue, red and green lines). The temperature is indicated by a thin gray line in the experiments with non-linear T(t).

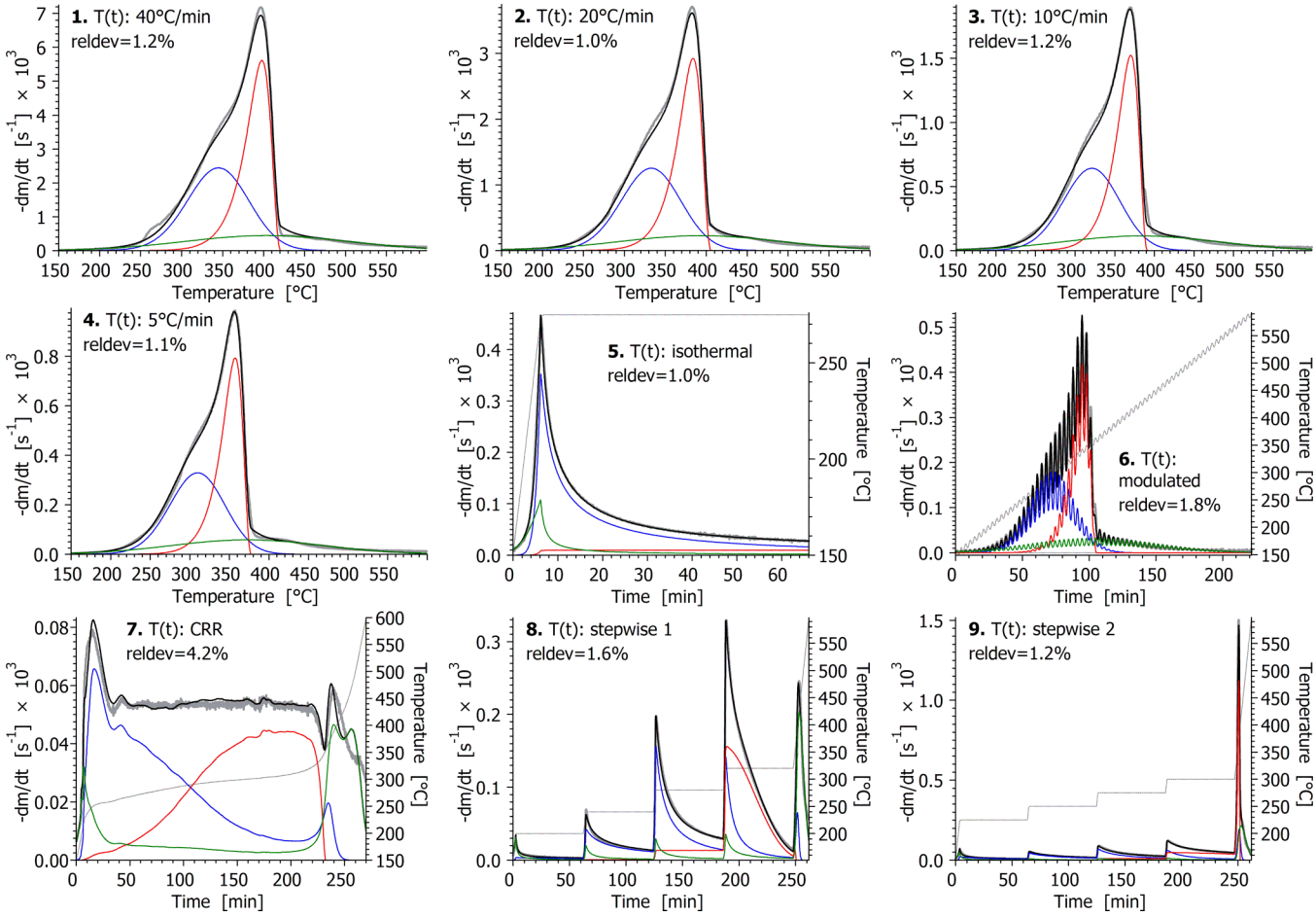

Figure 6. Results obtained for the spruce experiments by Evaluation **3** and Model Variant **III**. (See Figure 5 for the notations.)

The obtained kinetic parameters are listed in Table 3. For comparison we listed the corresponding values from two recent works on agricultural residues that employed similar kinetic models as well as a least squares evaluation of experiments with linear and non-linear T(t).[28,29] In this table E_1 and E_3 are the means of the corresponding activation energy distributions. The cellulose kinetics in the present work, however, differs from its predecessors: E_2 denotes an activation energy in the columns of Birch and Spruce while it is the mean of an activation energy distribution in the columns corresponding to the older works.

The kinetic parameters of the birch and spruce samples are close to each other. The difference between the two E_2 values is only 5 kJ/mol. The differences in the A_j values follow the differences in the E_j values due to the well-known compensation effect between E and A. The n_2 and z_2 values determine similar $f(\alpha_2)$ functions, as shown in Figure 4. This explains why the assumption of common E_2, n_2, and z_2 values resulted only in a slight increase of $reldev_{18}$ in Evaluation **4**.

Table 3: The parameters obtained in Evaluation 3 for Model Variant III and their comparison with earlier results[a]

Sample	Birch	Spruce	Four agri-cultural residues[b]	Two corn-cobs[c]
E_1 / kJ mol^{-1}	152	169	177	180
E_2 / kJ mol^{-1}	174	169	185	187
E_3 / kJ mol^{-1}	230	=	194	225
$\log_{10} A_1/s^{-1}$	11.58	12.62	<14.43>	<14.89>
$\log_{10} A_2/s^{-1}$	11.98	11.55	<13.77>	14.11
$\log_{10} A_3/s^{-1}$	16.33	16.11	<14.23>	16.25
σ_1 / kJ mol^{-1}	6.0	8.6	4.3	3.9
σ_2 / kJ mol^{-1}	n.a.	n.a.	1.9	0.2
σ_3 / kJ mol^{-1}	34.1	=	34.5	31.3
n_2	0.80	0.73	n.a.	n.a.
z_2	1.04	1.26	n.a.	n.a.
c_1	0.32	0.34	<0.10>	<0.22>
c_2	0.45	0.34	<0.33>	<0.32>
c_3	0.12	0.17	<0.29>	<0.18>

[a] Character '=' indicates parameter values that are identical for both woods. Brackets < > indicate averages. [b] Values obtained for corn stalk, rice husk, sorghum straw and wheat straw by Várhegyi et al.[28] [c] Values obtained for two corncob samples from different climates by Trninić et al.[29]

The Ej, σ_1 and σ_3 values obtained in the present work are comparable with the corresponding values from earlier work on straws and corncobs. The listed differences cannot be regarded high if we keep in mind the high ash content of the agricultural residues (1.5 – 16% vs. 0.2% in the present wood samples); the well-known differences in the composition of the hemicelluloses and lignin; the different model for the description of the cellulose decomposition; and the much wider range of T(t) functions in the present work.

3.5. Prediction tests. A usable model should predict approximately the behavior of the samples outside of the temperature programs at which the model parameters were determined. To test this feature, a narrower subset of the experiments can be evaluated, and, on this basis, predictions can be made for those experiments which were not included into the evaluation.[22,26,28,29] In the present work the experiments with temperature programs **4** – **9** were selected as a subset evaluated separately. Figures 5 and 6 show that these experiments produced the lowest decomposition rates in our dataset; the peaks of their $-\mathrm{d}m/\mathrm{d}t$ curves, $(-\mathrm{d}m/\mathrm{d}t)_{\mathrm{peak}}$, were in the range of 0.1×10^{-3} – 1×10^{-3} s^{-1}. The evaluation of these ten slow experiments by Model Variant **III** formed the basis for the prediction of experiments at temperature programs **1** – **3** (heating rates 10, 20, and 40°C/min) that had much higher decomposition rates: the peak of their $-\mathrm{d}m/\mathrm{d}t$ were in the range of 2×10^{-3} – 8×10^{-3} s^{-1}. It may be interesting to note that Evaluations **1** – **5** provided nearly the same fit qualities in the prediction tests. Figure 7 displays the results of these prediction tests by Evaluation **3**. As Figure 3 indicates, the fit quality depends on the range of the extrapolations: it is better at 10°C [when $(-\mathrm{d}m/\mathrm{d}t)_{\mathrm{peak}}\approx2\times10^{-3}$ s^{-1}] than at 40°C/min [when $(-\mathrm{d}m/\mathrm{d}t)_{\mathrm{peak}}\approx7\times10^{-3}$–$8\times10^{-3}$ s^{-1}]. Nevertheless, the simulated curves approximate reasonably the shape and position of the experimental $-\mathrm{d}m/\mathrm{d}t$ curves in all cases.

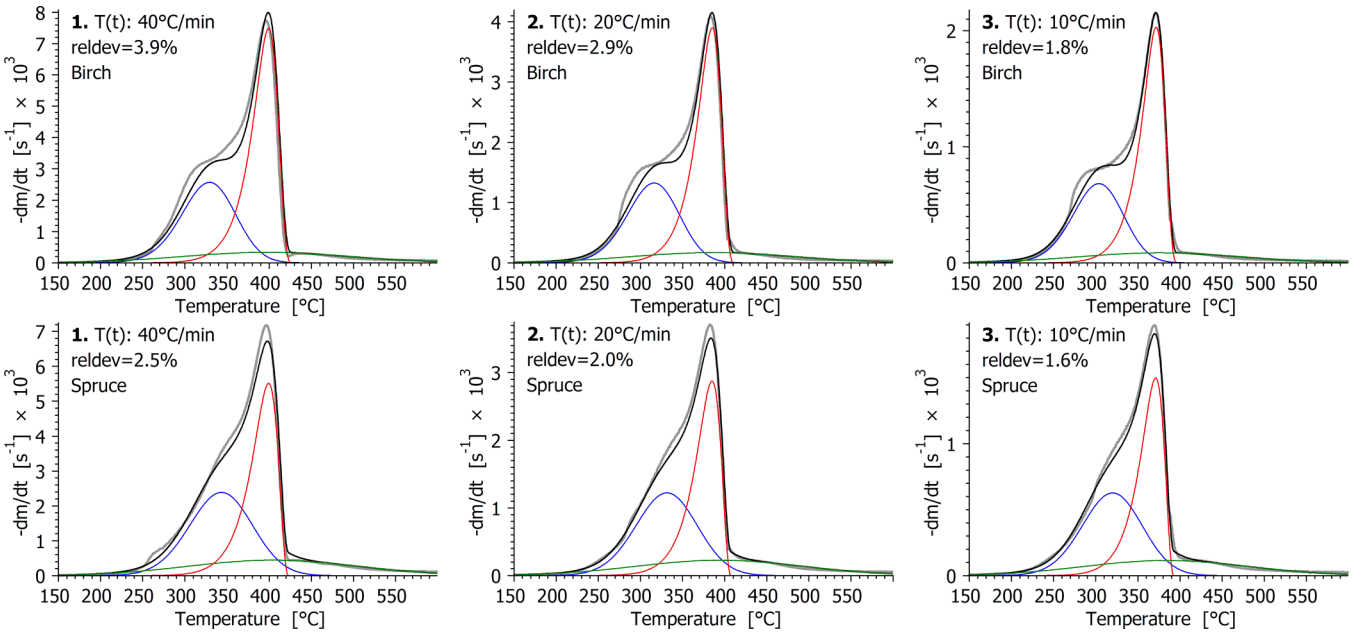

Figure 7. Predicting the faster experiments of the study using parameters obtained from the evaluation of ten slower experiments in Evaluation **3** by Model Variant **III**. (See Figure 5 for the notations.)

3.6. Modeling by *n*-order Kinetics. The *n*-order kinetics has the same number of model parameters as the DAEM with Gaussian distribution, while its numerical solution is simpler and faster. Its solution is also easier than that of equations 8 – 9. To test this approach, all evaluations were carried out by a model in which the decomposition of the pseudocomponents was described by *n*-order reactions (see eq 7 in paragraph 2.4).

The results are shown as Model Variant **IV** in Table 2. Model Variant **IV** provided nearly as good fit qualities as Model Variant **III** and the prediction tests outlined in paragraph 3.5 also gave similar relative deviations. Figure 8 shows the results obtained for the 40°C/min experiments in the evaluation and prediction tests by the model of *n*-order reactions using the assumptions of Evaluation **3**.

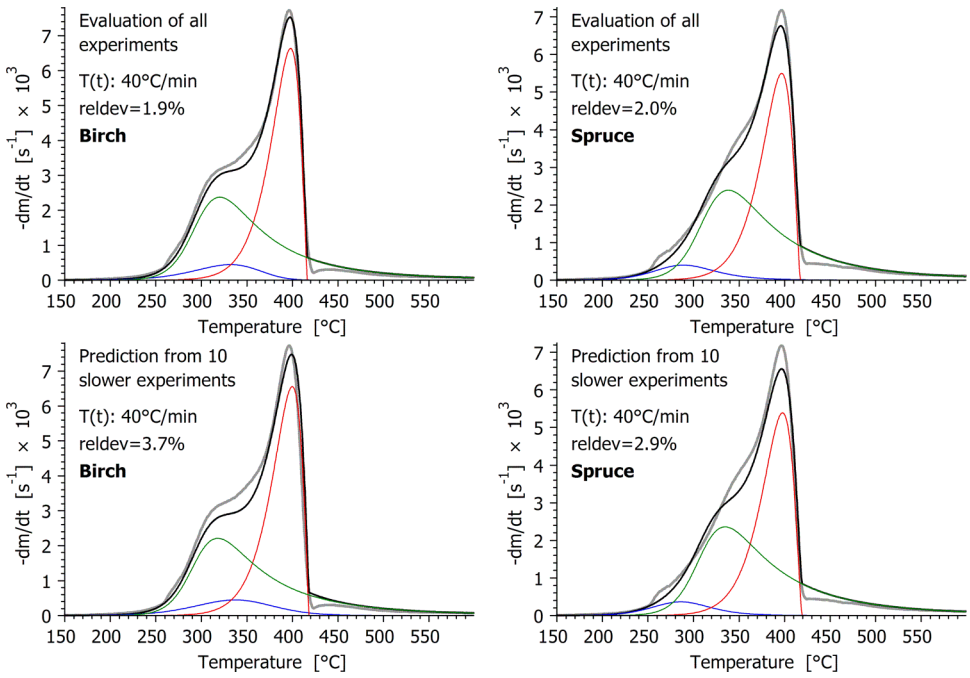

Figure 8. The 40°C/min experiments in the evaluation and prediction tests by Model Variant **IV** (n-order kinetics) in Evaluation **3**. (See Figure 5 for the notations.)

The most striking difference between Figure 8 and the corresponding parts of Figures 5 – 7 is the peculiar shape of the curve belonging to the third pseudocomponent (green line). This problem appeared in all the five evaluations with the n-order model. In Model Variants **I** – **III** the third pseudocomponent could be associated with the lignin decomposition and, at higher temperatures, with the slow carbonization of the char. In the present case, however, the decomposition of the hemicelluloses is also described mainly by pseudocomponent 3, as the peak maxima around 320–340°C of the green curves indicate in Figure 8. Accordingly pseudocomponent 3 describes most of the decomposition of the hemicelluloses plus the lignin pyrolysis plus the slow carbonization of the chars. This is a less clear reflection of the processes in the biomass pyrolysis than the ones expressed by the other model variants of the present study. Besides, the *n*-order kinetics describes the

complexity of the biomass materials in a rather formal way while a DAEM gives a simplified, but clear picture on the different reactivities of the different biomass species. The faster numerical calculation of the *n*-order kinetics has little importance nowadays, keeping in mind the low price and high speed of the modern desktop computers.

The corresponding kinetic parameters are listed in Table 4. A recent work on corncobs[29] and the work of Conesa and Domene[19] were used for comparison. The latter work studied five lignocellulosic biomasses: a Mediterranean sort of grass, wheat straw, an oceanic seaweed, and wastes from urban and agricultural pruning. There are several works in the biomass literature that describe the decomposition kinetics of the pseudocomponents with *n*-order reactions. The peculiarity of the work of Conesa and Domene was the allowing of high formal reaction order values. This line was followed later by Trninić et al. as well as in the present study. If the reaction order has a lower upper limit, e.g. it is forced to be less than 3, then more pseudocomponents are needed for a given fit quality than in the case of DAEM reactions.[26] The improvement is connected to the long tailing of a peak at high *n* that can formally approximate the slow, flat tailing sections of the DTG curves of lignocellulosic materials.

The activation energy values for the cellulose decomposition (E_2) are similar in Tables 3 and 4, as discussed in the next section. The other parameters are rather diverse. The parameters belonging to the birch and spruce samples are not far from each other in Table 4, but differ very much from the values reported for other biomasses as well as for the values in Table 3. The preexponential factors follow the activation energies, as usual. The very low preexponential factors for the cellulose decomposition in the article of Conesa and Domene appear to be misprints.

Table 4: The parameters obtained in Evaluation 3 for Model Variant IV and their comparison with earlier results[a]

Sample	Birch	Spruce	Two corn-cobs[b]	Five biomasses[c]
E_1 / kJ mol^{-1}	84	111	173	<195>
E_2 / kJ mol^{-1}	175	170	186	<189>
E_3 / kJ mol^{-1}	172	=	261	<157>
$\log_{10} A_1$/s^{-1}	5.54	8.70	<14.32>	<21.07>
$\log_{10} A_2$/s^{-1}	12.15	11.76	14.00	<7.04>
$\log_{10} A_3$/s^{-1}	13.63	13.16	19.52	<18.27>
n_1	1.07	2.07	1.90	<3.01>
n_2	0.58	0.61	0.94	<1.34>
n_3	4.71	=	10.38	<6.43>
c_1	0.06	0.05	0.27	n.a.
c_2	0.42	0.37	0.30	n.a.
c_3	0.41	0.44	0.16	n.a.

[a] Character '=' indicates parameter values that are identical for both woods. Brackets < > indicate averages. [b] Values obtained for two corncob samples from different climates by Trninić et al.[29] [c] Average values calculated from the results of Conesa and Domene on five lignocellulosic biomass materials.[19]

3.7. Notes on the Kinetics of the Cellulose Decomposition in the Biomass. The common element in Tables 3 and 4 is the similarities in the activation energy values of the cellulose decomposition, E_2. The E_2 values for the birch and spruce samples differ only by 1 kJ/mol between Tables 3 and 4. The cellulose activation energies taken from earlier works are also similar in Tables 3 and 4, though their range (185-189 kJ/mol) are higher than the ones obtained in the present study (169-175 kJ/mol). Nevertheless, these differences are not high, the lowest and highest E_2 values in Tables 3 and 4 differ by only 11%. The activation energies reported in the literature are obviously

much more diverse, but we selected for comparison only such works that employed models and evaluations similar to the present study.

In the present work 24 E_2 values were obtained in Evaluation **1** – **3** by Model Variants **I** – **IV**: 12 for birch and 12 for spruce. The birch values varied between 174.0 and 175.6 kJ/mol, while the spruce values were between 169.1 and 170.7 kJ/mol. Evaluation **4** and **5** by Model Variants **I** – **IV** yielded 8 E_2 values that were common for the birch and spruce samples; these values fell between 171.6 and 172.7 kJ/mol. Keeping in mind the differences in the modeling and the employed assumptions, the particularly narrow ranges of the E_2 values indicate that the experiments of the present work strongly determine this variable. We believe that this is connected to the particularly wide range of the employed T(t) programs that resulted in nearly a hundred times difference between the peak maxima of the slowest and the fastest experiments. The earlier works quoted in Tables 3 and 4 reported ca. 10% higher E_2 values, as noted above. It is possible that this difference is connected to their narrower range of T(t) programs.

3.8. Relevance to Torrefaction. As outlined in the Introduction, the aim of the present model was to describe the thermal decomposition both in the temperature domain of the torrefaction and at higher temperatures. The kinetics of the wood drying was not studied because most of the drying occurs before the start of the heating in the given apparatus, while the air is flushed out from the furnace.

One can calculate predicted values for characteristics of the torrefaction at any $T(t)$ function by the models presented:

(i) The normalized mass loss after the drying ($1-m(t)$);

(ii) The normalized mass loss due to the cellulose decomposition ($c_2\alpha_2(t)$);

(iii) The reacted fraction of the cellulose ($0\leq\alpha_2(t)\leq1$);

(iv) The normalized mass loss due to the non-cellulosic parts of the sample, which is the difference of 1-$m(t)$ and $c_2\alpha_2(t)$.

The term "normalized" means a division with the mass observed after the drying, as in the other parts of the article. Table 5 lists (i), (ii) and (iii) from the quantities listed above at various temperature – time values. For this table a 10°C/min heating and a subsequent isothermal section was assumed. The calculations were based on Model Variant **III**, using the parameters of Table 3.

The mass loss is higher for birch than for spruce at all temperature – time pairs of Table 5 (though the truncation to two decimals hides this at the lowest values). This can be due to the higher hemicellulose content of the birch wood.[3] As the data indicate, the devolatilization is negligible at 200°C. One can expect here only the decomposition of a small amount of thermally instable species, which may be enough to hinder the biological decay (rotting) but cannot increase the energy density of the obtained fuels. It may be interesting to observe that a 60-minute decomposition at 250°C and a 10-minute decomposition at 275°C result in nearly the same level of devolatilization for both woods. On the other hand, a prolonged heating at 275°C leads to a considerable loss of the cellulose component, which is not desired during torrefaction.

The comparison of the values in Table 5 with actual torrefaction data is left for a later work. Note that the temperature values in the present case were much closer to the actual temperatures than in a macro furnace or in an industrial reactor. Accordingly, care is needed for such a comparison.

Table 5: Simulated characteristics at various isothermal temperatures [a,b,c]

	0 min		10 min		30 min		60 min		120 min	
	Birch	Spruce	Birch	Spruce	Birch	Spruce	Birch	Spruce	Birch	Spruce
200°C										
1-$m(t)$	0.00	0.00	0.01	0.01	0.02	0.02	0.03	0.02	0.05	0.03
$c_2\alpha_2(t)$	0.00	0.00	0.00	0.00	0.00	0.00	0.00	0.00	0.00	0.00
$\alpha_2(t)$	0.00	0.00	0.00	0.00	0.00	0.00	0.00	0.00	0.00	0.00
225°C										
1-$m(t)$	0.01	0.01	0.03	0.03	0.07	0.04	0.10	0.06	0.14	0.09
$c_2\alpha_2(t)$	0.00	0.00	0.00	0.00	0.00	0.00	0.00	0.00	0.00	0.00
$\alpha_2(t)$	0.00	0.00	0.00	0.00	0.00	0.00	0.00	0.00	0.00	0.00
250°C										
1-$m(t)$	0.03	0.02	0.10	0.07	0.17	0.11	0.22	0.15	0.27	0.20
$c_2\alpha_2(t)$	0.00	0.00	0.00	0.00	0.00	0.00	0.01	0.01	0.01	0.01
$\alpha_2(t)$	0.00	0.00	0.00	0.00	0.01	0.01	0.01	0.02	0.03	0.03
275°C										
1-$m(t)$	0.08	0.06	0.22	0.16	0.30	0.24	0.35	0.30	0.42	0.38
$c_2\alpha_2(t)$	0	0.00	0.01	0.01	0.02	0.02	0.04	0.04	0.08	0.07
$\alpha_2(t)$	0	0.00	0.02	0.02	0.04	0.05	0.08	0.10	0.17	0.20
300°C										
1-$m(t)$	0.18	0.14	0.35	0.30	0.45	0.42	0.56	0.53	0.71	0.67
$c_2\alpha_2(t)$	0.00	0.00	0.04	0.03	0.10	0.09	0.20	0.17	0.34	0.28
$\alpha_2(t)$	0.01	0.01	0.08	0.10	0.23	0.26	0.44	0.49	0.76	0.83

[a] Model Variant **III** was used for prediction with the parameters of Table 3. [b] Isothermal torrefaction was assumed after a 10°C/min heating till the desired temperature. The time values in the header line belong to the isothermal section. [c] Three predicted torrefaction characteristics were tabulated at each temperature: the normalized mass loss [1-$m(t)$]; the normalized mass loss due to cellulose decomposition [$c_2\alpha_2(t)$]; and the reacted fraction of the cellulose [$\alpha_2(t)$].

4. CONCLUSIONS

(1) The thermal decomposition of a deciduous and an evergreen wood species were studied at slow heating programs, under well-defined conditions. Nine TGA experiments were carried out for

each sample with different temperature programs. Highly different temperature programs were selected to increase the information content available for the modeling. The ratio of the highest and lowest peak maxima was around 100 in the set of the experiments used for the evaluation. In this way the obtained models described the experiments in a wide range of experimental conditions.

(2) Several model variants were tested. The best performance was achieved when the cellulose decomposition was described by a submodel that can mimic self-acceleration tendencies. The decomposition of the non-cellulosic parts of the biomass was described by two reactions assuming a distributed activation energy model in this case. The complexity of the applied model reflects the complexity of the studied materials.

(3) The employed model contains 13 unknown parameters for a given biomass. Part of the kinetic parameters could be assumed common for the samples without a substantial worsening of the fit quality. This approach increased the average experimental information for an unknown parameter and revealed the similarities in the behavior of the different samples. In the preferred evaluation strategy of the paper the number of model parameters was close to the number of the evaluated DTG curves.

(4) When each partial reaction was described by *n*-order kinetics, similar fit qualities were obtained. However, the *n*-order kinetics describes the complexity of the biomass materials in a rather formal way.

(5) The results were checked by prediction tests. In these tests 10, 20 and 40°C/min experiments were simulated by the model parameters obtained from the evaluation of 10 experiments with lower reaction rates.

(6) A table was calculated by the preferred model variant that may provide guidance about the extent of devolatilization at various temperature – residence time values during wood torrefaction.

AUTHOR INFORMATION

Corresponding Author

* To whom correspondence should be addressed. E-mail: varhegyi.gabor@t-online.hu, Tel. +36 1 2461894, Fax: +36 1 4381147

ACKNOWLEDGMENT

The authors acknowledge the financial support by the Research Council of Norway and a number of industrial partners through the project STOP ("STable OPerating conditions for biomass combustion plants"). STOP is also a part of the research center CenBio (Bioenergy Innovation Centre).

NOMENCLATURE

α = reacted fraction of a component or pseudocomponent (dimensionless)

σ = width parameter (variance) of Gaussian distribution (kJ/mol)

A = pre-exponential factor (s^{-1})

E = activation energy (kJ/mol) or the mean of an activation energy distribution (kJ/mol)

f = empirical function (eq 9) expressing the change of the reactivity as the reactions proceed (dimensionless)

h_k = height of an experimental $-dm/dt$ curve (s^{-1})

m = the mass of the sample normalized by the initial dry sample mass (dimensionless)

n = reaction order (dimensionless)

of = objective function minimized in the least squares evaluation (dimensionless)

N_{exper} = number of experiments evaluated together by the method of least squares

N_k = number of evaluated data on the kth experimental curve

R = gas constant (8.3143×10^{-3} kJ mol^{-1} K^{-1})

reldev = the deviation between the observed and calculated data expressed as per cent of the corresponding peak height

$reldev_{18}$ = root mean square of the *reldev* values of 18 experiments

t = time (s)

T = temperature (°C, K)

z = formal parameter in eq 9 (dimensionless)

Subscripts:

i = digitized point on an experimental curve

j = pseudocomponent

k = experiment

REFERENCES

1. van der Stelt, M. J. C.; Gerhauser, H.; Kiel, J. H. A.; Ptasinski, K. J. Biomass upgrading by torrefaction for the production of biofuels: A review. *Biomass Bioenergy* **2011**, *35*, 3748-3762.

2. Chew, J. J.; Doshi, V. Recent advances in biomass pretreatment – Torrefaction fundamentals and technology. *Renew. Sustain. Energy Rev.* **2011,** 15, (8), 4212-4222.

3. Tapasvi, D.; Khalil, R. A.; Skreiberg, Ø.; Tran, K.-Q.; Gronli, M. G. Torrefaction of Norwegian birch and spruce – An experimental study using macro-TGA. *Energy Fuels* **2012**, *26*, 5232−5240.

4. Tapasvi, D. T., K-Q.; Wang, L.; Skreiberg, Ø.; Khalil, R. Biomass torrefaction – a review. *Proceedings of the 9th European Conference on Industrial Furnaces and Boilers, Estoril, Portugal* **2011**, (ISBN 978-972-99309-6-6).

5. Prins, M. J.; Ptasinski, K. J.; Janssen, F. J. J. G. Torrefaction of wood. *J. Anal. Appl. Pyrolysis* **2006,** *77*, 35-40.

6. Rousset, P.; Davrieux, F.; Macedo, L.; Perré, P. Characterisation of the torrefaction of beech wood using NIRS: Combined effects of temperature and duration. *Biomass Bioenergy* **2011,** 35, 1219-1226.

7. Melkior, T.; Jacob, S.; Gerbaud, G.; Hediger, S.; Le Pape, L.; Bonnefois, L.; Bardet, M. NMR analysis of the transformation of wood constituents by torrefaction. *Fuel* **2012,** 92, (1), 271-280.

8. Chen, W.-H.; Kuo, P.-C., Torrefaction and co-torrefaction characterization of hemicellulose, cellulose and lignin as well as torrefaction of some basic constituents in biomass. *Energy* **2011,** 36, (2), 803-811.

9. Prins, M. J.; Ptasinski, K. J.; Janssen, F. J. J. G. Torrefaction of wood. *J. Anal. Appl. Pyrolysis* **2006,** *77*, 28-34.

10. Chen, W.-H.; Kuo, P.-C., Isothermal torrefaction kinetics of hemicellulose, cellulose, lignin and xylan using thermogravimetric analysis. *Energy* **2011,** 36, (11), 6451-6460.

11. Bates, R. B.; Ghoniem, A. F., Biomass torrefaction: modeling of volatile and solid product evolution kinetics. *Bioresour Technol* **2012,** 124, 460-9.

12. Peng, J.; Bi, X. T.; Lim, J.; Sokhansanj, S. Development of torrefaction kinetics for British Columbia softwoods. *Inter. J. Chem. React. Eng.* **2012,** *10*, DOI:10.1515/1542-6580.2878.

13. Lu, K.-M.; Lee, W.-J.; Chen, W.-H.; Lin, T.-C. Thermogravimetric analysis and kinetics of co-pyrolysis of raw/torrefied wood and coal blends. *Applied Energy* **2013,** 105, 57-65.

14. Park, J.; Meng, J.; Lim, K. H.; Rojas, O. J.; Park, S., Transformation of lignocellulosic biomass during torrefaction. *J. Anal. Appl. Pyrolysis* **2013,** 100, 199-206.

15. Shang, L.; Ahrenfeldt, J.; Holm, J. K.; Barsberg, S.; Zhang, R.-z.; Luo, Y.-h.; Egsgaard, H.; Henriksen, U. B. Intrinsic kinetics and devolatilization of wheat straw during torrefaction. *J. Anal. Appl. Pyrolysis* **2013,** *100*, 145-152.

16. Blasi, C. D.; Lanzetta, M., Intrinsic kinetics of isothermal xylan degradation in inert atmosphere. *J. Anal. Appl. Pyrolysis* **1997,** 40-41 (1997), 287-303.

17. Várhegyi, G.; Antal, M. J., Jr.; Székely, T.; Szabó, P.: Kinetics of the thermal decomposition of cellulose, hemicellulose and sugar cane bagasse. *Energy Fuels* **1989**, *3*, 329-335.

18. Di Blasi, C. Modeling chemical and physical processes of wood and biomass pyrolysis. *Progr. Energy Combust. Sci.*, **2008**, *34,* 47-90.

19. Conesa, J. A.; Domene, A. Biomass pyrolysis and combustion kinetics through n-th-order parallel reactions. *Thermochim. Acta*, **2011**, *523*, 176-181.

20. Burnham, A. K.; Braun, R. L. Global kinetic analysis of complex materials. *Energy Fuels* **1999**, *13*, 1-22.

21. Avni, E.; Coughlin, R. W.; Solomon P. R., King H. H. Mathematical modelling of lignin pyrolysis. *Fuel* **1985**, *64* 1495-1501.

22. Várhegyi, G.; Szabó, P.; Antal, M. J., Jr. Kinetics of charcoal devolatilization. *Energy Fuels* **2002**, *16*, 724-731.

23. de Jong, W; Pirone, A; Wojtowicz, M. A. Pyrolysis of Miscanthus Giganteus and wood pellets: TG-FTIR analysis and reaction kinetics. *Fuel,* **2003**, *82*, 1139-1147.

24. Wójtowicz, M. A.; Bassilakis, R.; Smith, W. W.; Chen, Y.; Carangelo, R. M. Modeling the evolution of volatile species during tobacco pyrolysis. *J. Anal. Appl. Pyrolysis*, **2003**, *66*, 235-261.

25. Yi, S-C.; Hajaligol, M. R. Product distribution from the pyrolysis modeling of tobacco particles. *J. Anal. Appl. Pyrolysis*, **2003**, *66*, 217-234.

26. Becidan, M.; Várhegyi, G.; Hustad, J. E.; Skreiberg, Ø.: Thermal decomposition of biomass wastes. A kinetic study. *Ind. Eng. Chem. Res.* **2007**, *46*, 2428-2437.

27. Várhegyi, G.; Czégény, Zs.; Jakab, E.; McAdam, K.; Liu, C. Tobacco pyrolysis. Kinetic evaluation of thermogravimetric – mass spectrometric experiments. *J. Anal. Appl. Pyrolysis* **2009**, *86*, 310-322.

28. Várhegyi, G.; Bobály, B.; Jakab, E.; Chen, H.: Thermogravimetric study of biomass pyrolysis kinetics. A distributed activation energy model with prediction tests. *Energy Fuels,* **2011**, *25,* 24-32.

29. Trninić, M.; Wang, L.; Várhegyi, G.; Grønli, M.; Skreiberg, Ø.: Kinetics of corncob pyrolysis. *Energy Fuels,* **2012**, *26, 2005-2013.*

30. Manyà, J. J.; Velo, E.; Puigjaner, L. Kinetics of biomass pyrolysis: A reformulated three-parallel-reactions model. *Ind. Eng. Chem. Res.* **2003**, *42*, 434-441.

31. Tapasvi, D.; Khalil, R.; Várhegyi, G.; Skreiberg, Ø.; Tran, K.-Q.; Grønli, M. Kinetic behavior of torrefied biomass in an oxidative environment. *Energy Fuels,* **2013**, *27*, 1050-1060.

32. High resolution thermogravemetric analysis - A new technique for obtaining superior analytical results. TA Instruments report TA-023. Available at: http://www.tainstruments.co.jp/application/pdf/Thermal_Library/Applications_Briefs/TA023.PDF

33. Grønli, M. G.; Várhegyi, G.; Di Blasi, C.: Thermogravimetric analysis and devolatilization kinetics of wood. *Ind. Eng. Chem. Res.* **2002**, *41*, 4201-4208.

34. Várhegyi, G.; Chen, H.; Godoy, S. Thermal decomposition of wheat, oat, barley and Brassica carinata straws. A kinetic study. *Energy Fuels* **2009**, *23*, 646-652.

35. Várhegyi, G.; Szabó, P.; Mok W. S. L., Antal, M. J., Jr. Kinetics of the thermal decomposition of cellulose in sealed vessels at elevated pressures. Effects of the presence of water on the reaction mechanism. *J. Anal. Appl. Pyrolysis* **1993**, *26*, 159-174.

36. Donskoi, E.; McElwain, D. L. S. Optimization of coal pyrolysis modeling. *Combust. Flame* **2000**, *122*, 359-367.

37. de Jong, W.; Di Nola, G.; Venneker, B. C. H.; Spliethoff, H.; Wójtowicz, M. A. TG-FTIR pyrolysis of coal and secondary biomass fuels: Determination of pyrolysis kinetic parameters for main species and NOx precursors. *Fuel,* **2007**, *86*, 2367-2376.

38. Conesa, J. A.; Caballero, J. A.; Marcilla, A.; Font, R. Analysis of different kinetic models in the dynamic pyrolysis of cellulose. *Thermochim. Acta* **1995**, *254*, 175–192.

39. Capart, R.; Khezami, L.; Burnham, A. K. Assessment of various kinetic models for the pyrolysis of a microgranular cellulose. *Thermochim. Acta* **2004**, 417, 79–89.

40. Várhegyi, G.; Sebestyén, Z.; Czégény, Z.; Lezsovits, F.; Könczöl, S.: Combustion kinetics of biomass materials in the kinetic regime. *Energy Fuels,* **2012**, *26*, 1323-1335.

41. Várhegyi, G.; Szabó, P.; Jakab, E.; Till, F.; Richard J-R. Mathematical modeling of char reactivity in Ar-O2 and CO2-O2 mixtures. *Energy Fuels* **1996**, *10*, 1208-1214.